

Three different signal amplification strategies for the impedimetric sandwich detection of thrombin

*Cristina Ocaña and Manel de Valle**

*Sensors and Biosensors Group, Department of Chemistry, Universitat Autònoma de Barcelona,
Edifici Cn, 08193 Bellaterra, Barcelona, SPAIN*

Abstract

In this work, we report a comparative study on three highly specific amplification strategies for the ultrasensitive detection of thrombin with the use of aptamer sandwich protocol. The protocol consisted on the use of a first thrombin aptamer immobilized on the electrode surface, the recognition of thrombin protein, and the reaction with a second biotinylated thrombin aptamer forming the sandwich. Through the exposed biotin end, three variants have been tested to amplify the electrochemical impedance signal. The strategies included (a) silver enhancement treatment, (b) gold enhancement treatment and (c) insoluble product produced by the combination of the enzyme horseradish peroxidase (HRP) and 3-amino-9-ethylcarbazole (AEC). The properties of the sensing surface were probed by electrochemical impedance measurements in the presence of the redox marker ferrocyanide/ferricyanide. Insoluble product strategy and silver enhancement treatment resulted in the lowest detection limit of the probe (0.3pM), while gold enhancement method resulted in highest reproducibility, 8.8% RSD at pM thrombin concentration levels. Results of silver and gold enhancement treatment also permitted direct inspection by scanning electron microscopy (SEM).

Keywords : aptamer, impedance, gold nanoparticles, amplification, aptasensor, insoluble product.

1.Introduction

Aptamers are single-stranded nucleic acid molecules that can bind with high affinity and specificity to a wide range of target molecules, such as drugs, proteins, or even whole cells (Jayasena 1999; Patel and Suri 2000). They are generated by an in vitro selection process called SELEX (Ellington and Szostak 1990). This method allows the identification of a unique RNA/DNA molecules from very large population of random sequence oligomers, which bind to the target molecule with very high affinity and specificity. They show dissociation constant typically from the micromolar to low picomolar range, comparable to those of some monoclonal antibodies (Jenison et al. 1994). Not surprisingly, aptamers have found growing interest as active separation materials in chromatography (Kotia et al. 2000), and electrophoresis (Clark and Remcho 2002), as therapeutic (Biesecker et al. 1999; Hicke et al. 2001) or diagnostic agents, and as active materials for biosensing (Evtugyn et al. 2012). The use of aptamers as recognition elements in biosensing to form aptasensors offers, over classical affinity sensing methods, mainly based on antibodies, a multitude of advantages, such as the possibility of easily regenerating the function of immobilized aptamers, their easy and homogenous preparation and the possibility of using them without labelling.

Among aptasensors, different transduction techniques can be used; optical(Lee and Walt 2000), atomic force microscope (Basnar et al. 2006), surface plasmon resonance (Vasilescu et al. 2013), electrochemical (Ocaña et al. 2012; Radi et al. 2005) and piezoelectric (Srijanto et al. 2012). In the last years, among the different electrochemical techniques reported, the use of electrochemical impedance spectroscopy (EIS) has grown among the examined literature (McDonald 1987). EIS is a characterization technique which is very sensitive to changes of the interfacial properties of modified electrodes upon biorecognition events taking place at the electrode surface (Bardea et al. 1999; Loo et al. 2012). Other important features presented by EIS are that it does not require any special reagent for the analysis, it has the capacity for label-free detection and it is a sensitive and cost-efficient technique.

Nowadays, since many small target analytes are present at ultralow-levels, there are increasing demands for ultrasensitive detection. Nevertheless, it is sometimes difficult to obtain ultrasensitive detection of small targets. Thus, in order to reach the ever more demanding detection limits, the exploration of novel amplification strategies is essential

(Bonanni and del Valle 2010). Different amplification variants have been used in affinity biosensors, such as the use of gold nanoparticles (Bonanni et al. 2008; Yuan et al. 2014), silver nanoparticles (Song et al. 2014), the coupling with enzymatic reactions (Kaatze et al. 2012; Zheng et al. 2014), or the use of graphene (Bai et al. 2014) or carbon nanotubes (Zhang et al. 2013) as labels carriers.

In this work, we report a comparative study on three highly specific amplification strategies for the ultrasensitive detection of thrombin with the use of aptamer sandwich protocol. The strategies included (a) silver enhancement treatment, (b) gold enhancement treatment and (c) insoluble product produced by the combination of the enzyme horseradish peroxidase (HRP) and 3-amino-9-ethylcarbazole (AEC). The protocol consisted on the use of a first thrombin aptamer immobilized on the electrode surface, the recognition of thrombin protein, and the reaction with a second biotinylated thrombin aptamer forming the sandwich. Through the exposed biotin end, the three amplification variants have been tested to as enhancers of the electrochemical impedance signal.

2. Experimental

2.1. Chemicals

Potassium dihydrogen phosphate, potassium ferricyanide $K_3[Fe(CN)_6]$, potassium ferrocyanide $K_4[Fe(CN)_6]$, sodium monophosphate, streptavidin gold nanoparticles, avidin horseradish peroxidase conjugate (Av-HRP), 3-amino-9-ethylcarbazole, 655nm streptavidin quantum dots (strep-QDs), avidin and the target protein thrombin (Thr), were purchased from Sigma (St. Louis, MO, USA). Poly(ethylene glycol) 1000 (PEG), sodium chloride and potassium chloride were purchased from Fluka (Buchs, Switzerland). LI silver enhancement kit was obtained from Nanoprobes (Yaphank, New York). All-solid-state avidin-modified electrodes (AvGECs) were prepared using 50 μ m particle size graphite powder (Merck, Darmstadt, Germany), Epotek H77 resin and its corresponding hardener (were both from Epoxy Technology, Billerica, MA, USA), and avidin. All reagents were analytical reagent grade. Aptamers used in this study were synthesized on demand by Sigma Aldrich (St. Louis, MO, USA). Stock solutions of

1 aptamers were diluted with sterilized and deionised water, separated into fractions and
2 stored at -20°C until required. Their base sequences were:

- 3 • AptThrBio1: 5'-GGTTGGTGTGGTTGG-Biotin-3'
- 4 • AptThrBio2: 5'-Biotin-AGTCCGTGGTAGGGCAGGTTGGGGTGACT-3'
- 5 • AptCytC: 5'-Biotin-
6 AGTGTGAAATATCTAAACTAAATGTGGAGGGTGGGACGCGGAAGAAG
7 TTTATTTTTCACACT-3'

8 All solutions were made up using Milli-Q water from Milli-Q System (Millipore,
9 Billerica, MA, USA). The buffers employed were: PBS (187 mM NaCl, 2.7 mM KCl,
10 8.1 mM $\text{Na}_2\text{HPO}_4 \cdot 2\text{H}_2\text{O}$, 1.76 mM KH_2PO_4 , pH 7.0), acetate buffer 0.5M (pH 5.5),
11 10nM PBS without NaCl and KCl.

22 2.2. Apparatus

23 AC impedance measurements were performed with the aid of an Autolab PGStat 20
24 (Metrohm Autolab B.V, Utrecht, The Netherlands). FRA (Metrohm Autolab) software
25 was used for data acquisition and control of the experiments. A three electrode
26 configuration was used to perform the impedance measurement: a platinum-ring
27 auxiliary electrode (Crison 52–67 1, Barcelona, Spain), a Ag/AgCl reference electrode
28 and the constructed AvGEC as the working electrode. A scanning electron microscope
29 (SEM) (Merlin, Zeiss, Germany) was used to visualize silver and gold enhanced strep-
30 AuNPs on electrode surface. Temperature-controlled incubations were done using an
31 Eppendorf Thermomixer 5436.

32 2.3. Construction of working electrodes

33 The avidin-modified electrodes were prepared using a PVC tube body (6 mm i.d.) and a
34 small copper disk soldered to the end of an electrical connector. Avidin modification
35 was employed for further immobilization of proper aptamer by affinity reaction. The
36 conductive part of AvGECs was an avidin epoxy graphite conductive paste, formed
37 from graphite (18%), avidin (2%) and epoxy resin (80%), which was deposited into the
38 cavity in the plastic body, filling it (Bonanni et al. 2007). The composite material was
39 cured in an oven at 40°C for 7 days. Before each use, the electrode surface was

1 moistened with Milli-Q water and then thoroughly smoothed with abrasive sandpaper
2 and finally with alumina paper (polishing strips 301044-001, Orion) in order to obtain a
3 reproducible electrochemical surface (Lermo et al. 2007; Williams et al. 2003).
4
5
6
7
8

9 **2.4. Protein capture and amplification protocols**

10
11 The scheme of experimental protocols for thrombin analysis, described in detail below,
12 is represented in Fig. 1.
13
14
15

16 **2.4.1. Aptamer immobilization**

17
18 The first step consists of aptamer AptThrBio1 immobilization on the electrode surface.
19 A volume of 160 μL of MilliQ water containing 35 pmols of aptamer solution was
20 heated to 80–90 $^{\circ}\text{C}$ for 3 minutes in order to promote the loose conformation of the
21 aptamer. Then, the solution was dipped in a bath of cold water and the electrode was
22 immersed in it, where the avidin-biotin affinity interaction took place for 15 minutes at
23 the electrode surface. This was followed by two washing steps using PBS buffer
24 solution for 10 minutes, in order to remove any unadsorbed aptamer.
25
26
27
28
29
30
31
32

33 **2.4.2. Blocking step**

34
35 To avoid any possible nonspecific adsorption, the electrodes were dipped in 160 μL of
36 PEG 40 mM. This was followed by two washing steps using PBS buffer solution for 10
37 minutes.
38
39
40
41

42 **2.4.3. Thrombin detection**

43
44 The electrodes were dipped in a solution with the desired concentration of Thr. The
45 incubation took place for 15 minutes. Then, the biosensors were washed twice with PBS
46 buffer solution for 10 minutes.
47
48
49
50

51 **2.4.4. Sandwich formation**

52
53 In order to obtain the aptamer sandwich formation, the electrodes were dipped in 160 μL
54 of PBS solution containing 12 pmols of AptThrBio2. The incubation took place for 15
55 minutes. This was followed by two washing steps using PBS buffer solution for 10
56 minutes.
57
58
59
60
61
62
63
64
65

2.4.5 Amplification Protocols

Three different variants were used;

Silver enhancement treatment (Ocaña and Del Valle 2014)

AvGEC electrodes modified with the sandwich complex were incubated in 160 μ L of strep-AuNPs, from a 1/100 dilution of the stock solution in PBS buffer. The reaction tube was incubated at 25°C with gentle stirring for 20 minutes. This step was followed by two gentle washing steps in PBS buffer for 10 minutes at 25°C. Negative controls were performed for the strep-AuNPs addition step using AptCytC as aptamer without affinity.

20 μ L of a solution obtained by the combination of 10 μ L of enhancer and 10 μ L of initiator were deposited onto the electrode surface and left for 7 minutes to facilitate the reaction. Silver enhancement occurs during the catalytic reduction of silver from one solution (e.g. the enhancer) by another (e.g. the initiator) in the presence of gold nanoparticles. The reduction reaction causes silver to build up on the surface of the gold nanoparticles. After this catalytic silver reduction, the electrodes were thoroughly washed with deionized water to stop the reaction. The silver enhancing solution was prepared immediately before each use. For silver enhancement treatment, the negative control used was a non-biotinylated AptCytC as aptamer without affinity.

Gold enhancement treatment

AvGEC electrodes modified with the sandwich complex were incubated in 160 μ L of strep-AuNPs, from a 1/100 dilution of the stock solution in PBS buffer. The reaction tube was incubated at 25°C with gentle stirring for 20 minutes. This step was followed by two gentle washing steps in PBS buffer for 10 minutes at 25°C. Negative controls were performed for the strep-AuNPs addition step using AptCytC as aptamer without affinity.

The modified electrodes after the sandwich protocol and strep-AuNPs fixation were further immersed in a solution containing a mixture of 0.01% HAuCl₄ and 0.4 mM NH₂OH·HCl (pH 6.0) for 2 min at 25°C, rinsed, and then treated for 2 additional min. In

order to prevent the non-specific background of fine gold particles, the electrodes were rinsed with a solution of 0.6 M triethylammonium bicarbonate buffer after each amplification. Solutions were freshly prepared in a lightproof container before each use.

Insoluble product treatment

AvGEC electrodes modified with the sandwich complex were incubated in 160 μ L of av-HRP enzyme conjugate, from a 1/500 dilution of the stock solution in PBS buffer, during 30 minutes with gentle stirring. This step was followed by two gentle washing steps in PBS buffer for 10 minutes at 25°C.

10 mg of AEC were dissolved in 1mL of DMF (yellow color). Then, 66 μ L of the previous solution were mixed in 2mL of acetate buffer 0.5M (pH 5.5). After that, 66 μ L of H₂O₂ 0.3% was added to the previous solution. Finally, 20 μ L of this solution were deposited onto the electrode surface for 15 minutes, a red product was formed onto the electrode surface, Figure 2. This step was followed by two washing steps with distilled water.

Different selectivity experiments carried out were performed with the same protocols unless where specified.

All incubations were carried out at controlled temperature in the thermomixer.

2.5. Impedimetric detection

Impedance experiments were carried out at an applied potential of 0.17V (vs. Ag/AgCl reference electrode), with a range of frequency of 50KHz-0.05Hz, an AC amplitude of 10 mV and a sampling rate of 10 points per decade above 66 Hz and 5 points per decade at the lower range. All measurements were performed in PBS buffer containing 0.01M K₃[Fe(CN)₆]/K₄[Fe(CN)₆] (1:1) mixture, used as a redox marker. The impedance spectra were plotted in the form of complex plane diagrams (Nyquist plots, $-Z_{im}$ vs. Z_{re}) and fitted to a theoretical curve corresponding to the equivalent circuit with Z_{view} software (Scribner Associates Inc., USA).

3. Results

The modification of the electrodes surface with the sandwich formation as well as the three different amplification strategies were studied by electrochemical impedance spectroscopy using a solution of $K_3[Fe(CN)_6]$ / $K_4[Fe(CN)_6]$ as a redox marker in the bulk solution.

Typical spectral obtained in these experiments are shown in Figure 3. The corresponding equivalent circuit was formed by one resistor/ capacitor element in series with a resistance. In it, the resistance in series with the capacitor element, R_s , corresponds to the resistance of the solution, the resistance in parallel with the capacitor element, R_{ct} , is the charge transfer resistance between the solution and the electrode surface, whilst the capacitor element, here a constant phase element (CPE), is associated with the double-layer capacitance. The use of a CPE instead of a capacitor is required to optimize the fit to the experimental data, and this is due to the nonideal nature of the electrode surface. For all performed fittings, the chi-square goodness-of-fit test was thoroughly checked to verify calculations. In all cases, calculated values for each circuit remained in the range of 0.0003-0.15 much lower than the tabulated value for 50 degrees of freedom (67.505 at 95% confidence level). Thus demonstrating the high significance of the final fits.

The parameter of interest in our case is represented by the charge transfer resistance R_{ct} . This value in the Nyquist plot corresponds to the diameter of the semicircle. In order to compare the results obtained from the different electrodes used, and to obtain independent and reproducible results, a relative transformation of signals was needed (Bonanni et al. 2006). Thus, the Δ_{ratio} value was defined according to the following equations:

$$\Delta_{ratio} = \Delta_s / \Delta_p$$

$$\Delta_s = R_{ct} \text{ (AptThrBio1-Thr/AptThrBio2/strep-AuNPs or Av-HRP/silver enhance. or gold enhance. or insoluble product) } - R_{ct} \text{ (electrode-buffer)}$$

$$\Delta_p = R_{ct} \text{ (AptThrBio1) } - R_{ct} \text{ (electrode-buffer)}$$

where $R_{ct} \text{ (AptThrBio1-Thr/AptThrBio2/strep-AuNPs or Av-HRP/silver enhance. or gold enhance. or insoluble product)}$ was the electron transfer resistance value measured after thrombin incubation, sandwich

formation and different signal amplification methods; $R_{ct(AptThrBio1)}$ was the electron transfer resistance value measured after aptamer immobilization on the electrode, and $R_{ct(electrode-buffer)}$ was the electron transfer resistance of the blank electrode and buffer.

As can be seen in Fig. 3, the R_{ct} value increased after each biosensing step. This change was due to the inhibition of the electrochemical reaction of the redox marker at the electrode surface, caused by the presence of blocking layers. Two different factors should be taken into account to properly explain this effect: electrostatic repulsion and sterical hindrance. The former is more significant in the first step of protocol; when the AptThrBio1 is immobilized onto the electrode surface by avidin–biotin affinity, a first layer is formed, where negatively charged phosphate groups of DNA aptamer skeleton are responsible of electrostatic repulsion of the negatively charged redox marker, thus inhibiting the interfacial transfer process and resulting in R_{ct} increment. The addition of Thr and a second AptThrBio2 to form a sandwich complex results in a further increment of R_{ct} due to the increased quantity of negative charge and the hindrance caused by the formation of a double layer. In Fig. 3a) and b), after the addition of strep-AuNPs an increment of R_{ct} value was clearly seen because of the increased space resistance due to gold streptavidin conjugates. In addition, working at pH 7, streptavidin is slightly negatively charged (pI is around pH 5) and this fact also contributes to enhancement of impedance (Sivasankar et al. 1998). In the second amplification step, silver or gold enhancement treatment (Cai et al. 2002; Hanaee et al. 2007), significant increments of R_{ct} values were also observed and attributable to the catalytic silver or gold deposition on gold, respectively. In the case of silver treatment, the obtained increment of R_{ct} is higher than in the gold enhancement, probably because silver deposition mechanism is faster than gold deposition mechanism.

As can be seen in Fig 3c), after the addition of av-HRP in insoluble product strategy, an increment of R_{ct} was produced, in this case probably attributed to the sterical hindrance because of the size of the superimposed enzyme molecule. After the enzymatic reaction step, R_{ct} showed a higher significant increase which indicates that the deposition of the formed insoluble product has a big effect on the charge transfer reaction, though the development of a clear insulating layer.

Detection of thrombin: comparison between three different amplification strategies

The aim of these experiments was to study and compare the best amplification technique using a sandwich protocol. All steps of these experiments have been optimized separately (data not shown). The obtained calibration curves are represented in Fig. 4. As can be seen in this figure, all calibration curves increased until the value of 100pM of Thr, this could be due to the fact that concentrations larger than 100pM cause a saturation on the electrode surface.

The first amplification method used was silver enhancement treatment. This well-known method is based on the deposition of metallic silver after the addition of strep-AuNP in the sandwich aptamer modified electrode. This strategy presented high sensitivity and reproducibility.

Secondly, the amplification method used was gold enhancement treatment. This method is based on the same protocol which have just explained before, in this case with gold deposition. This protocol showed high reproducibility and sensitivity.

Finally, the last amplification strategy used was insoluble product treatment. This method is focused on the production of an insoluble product by an enzymatic reaction. These reagents are converted to water and insoluble product, which precipitate and cause a blocking of the electrode surface, producing a high increment of R_{ct} . This strategy presented the highest sensitivity and lowest detection limit.

All numerical results are represented in Table 1. The highest sensitivity was attained using insoluble product reaction due to the fast blocking of the electrode surface, while showing the lowest reproducibility value. In addition, this method together with the silver enhancement treatment showed the lowest detection limit of the target analyte, 0.3 pM, demonstrating that these methods presented ultrahigh sensitivity for the detection of thrombin. Moreover, a signal increment of up to 189 % between simple biosensing and insoluble product strategy was observed, but with requirements of 15 min amplification time. However, gold enhancement treatment showed the best reproducibility value, 8.8%RSD. This confirm that silver enhancement and insoluble product strategies may reach a low detection limit and ultrahigh sensitivity for thrombin detection.

Scanning Electron Microscope characterization

In order to confirm the presence and distribution of gold nanoparticles onto the electrode surface with silver and gold enhancement treatment, SEM images were taken. These experiments also provided an image of the homogeneity and accessibility of the anchorage points supplied by the avidin entrapped in the biocomposite. SEM images taken at an acceleration voltage of 3 kV are shown in Figure 6. Figure 6 a.1) and a.2) showed positive and negative control with the use of silver enhancement method, while Figure 6 b.1) and 6 b.2) showed positive and negative controls of gold enhancement treatment. As can be seen, both positive controls showed a quite homogeneous distribution of the nanoparticles. That fact also implies a regular distribution of avidin molecules in the biocomposite and a well-organized formation of aptamer sandwich onto the electrode surface. While silver enhancement treatment showed monocrystalline particles, gold enhancement treatment showed sphere nanoparticles, this could be due to the fact that silver crystallized in specific directions thanks to the disposition of the streptavidin around of gold nanoparticles. Comparing these experiments with their respective negative controls that did not use the biotinylated complementary target aptamer, a surface without nanoparticles can be observed.

Selectivity of the aptamer sandwich protocol

Selectivity of each amplification strategy was examined by challenging thrombin with different possible interfering proteins. Prothrombin, IgG, fibrinogen, BSA and cytochrome c were employed to investigate the specificity of the three methods for the detection of thrombin. As shown in Figure 7, it is observed that incubation with these proteins produced negligible response compared with 75pM Thr even at concentration four or five orders of magnitude higher than typical Thr serum concentration, demonstrating that the three signal amplification methods possessed sufficient specificity for thrombin detection.

4. Conclusions

In this study, three different signal amplification strategies were studied and compared for the ultrasensitive impedance detection of thrombin (silver enhancement treatment, gold enhancement treatment and insoluble product reaction produced by the combination of HRP and AEC).

With the different strategies reported, low detection limits in the pM level, ample range of responses for thrombin concentration and low % RSD values were achieved. Among the three methods proposed, insoluble product reaction and silver enhancement treatment were the best overall methods displaying low detection limits, 0.3 pM, and high affinities with a sensitivity values of $7.0 \cdot 10^{-14} \text{ M}^{-1}$ and $2.2 \cdot 10^{-14} \text{ M}^{-1}$ respectively. In addition, all the methods assayed showed high selectivity values. The silver and gold enhancement treatment also permitted to visualize the gold nanoparticles on the electrode surface with SEM. This allowed confirming the proposed steps of the protocol and a homogeneous distribution of biosensing sites on the electrodes.

Acknowledgments

The authors acknowledge financial support from the Spanish Ministry of Economy and Innovation (MINECO, project CTQ2013-41577-P). Manel del Valle thanks the support from the Catalonia program ICREA Academia.

References

- Bai, L., Chai, Y., Pu, X., Yuan, R., 2014. A signal-on electrochemical aptasensor for ultrasensitive detection of endotoxin using three-way DNA junction-aided enzymatic recycling and graphene nanohybrid for amplification. *Nanoscale* 6(5), 2902-2908.
- Bardea, A., Patolsky, F., Dagan, A., Willner, I., 1999. Sensing and amplification of oligonucleotide-DNA interactions by means of impedance spectroscopy: a route to a Tay-Sachs sensor. *Chem. Comm.*(1), 21-22.
- Basnar, B., Elnathan, R., Willner, I., 2006. Following aptamer-thrombin binding by force measurements. *Analytical Chemistry* 78(11), 3638-3642.
- Biesecker, G., Dihel, L., Enney, K., Bendele, R.A., 1999. Derivation of RNA aptamer inhibitors of human complement C5. *Immunopharmacology* 42(1-3), 219-230.

1 Bonanni, A., del Valle, M., 2010. Use of nanomaterials for impedimetric DNA sensors: A review.
2 Analytica Chimica Acta 678(1), 7-17.

3 Bonanni, A., Esplandiu, M.J., del Valle, M., 2008. Signal amplification for impedimetric
4 genosensing using gold-streptavidin nanoparticles. Electrochimica Acta 53(11), 4022-4029.

5
6 Bonanni, A., Esplandiu, M.J., Pividori, M.I., Alegret, S., del Valle, M., 2006. Impedimetric
7 genosensors for the detection of DNA hybridization. Anal. Bioanal. Chem. 385(7), 1195-1201.

8
9 Bonanni, A., Pividori, M.I., del Valle, M., 2007. Application of the avidin-biotin interaction to
10 immobilize DNA in the development of electrochemical impedance genosensors. Anal. Bioanal.
11 Chem. 389(3), 851-861.

12
13 Cai, H., Wang, Y.Q., He, P.G., Fang, Y.H., 2002. Electrochemical detection of DNA hybridization
14 based on silver-enhanced gold nanoparticle label. Analytical Chimica Acta 469(2), 165-172.

15
16 Clark, S.L., Remcho, V.T., 2002. Aptamers as analytical reagents. Electrophoresis 23(9), 1335-
17 1340.

18
19 Ellington, A.D., Szostak, J.W., 1990. In vitro selection of RNA molecules that bind specific
20 ligands. Nature 346(6287), 818-822.

21
22 Evtugyn, G.A., Kostyleva, V.B., Porfireva, A.V., Savelieva, M.A., Evtugyn, V.G., Sitdikov, R.R.,
23 Stoikov, I.I., Antipin, I.S., Hianik, T., 2012. Label-free aptasensor for thrombin determination
24 based on the nanostructured phenazine mediator. Talanta 102(0), 156-163.

25
26 Hanaee, H., Ghourchian, H., Ziaee, A.A., 2007. Nanoparticle-based electrochemical detection of
27 hepatitis B virus using stripping chronopotentiometry. Analytical Biochemistry 370(2), 195-200.

28
29 Hicke, B.J., Marion, C., Chang, Y.F., Gould, T., Lynott, C.K., Parma, D., Schmidt, P.G., Warren, S.,
30 2001. Tenascin-C aptamers are generated using tumor cells and purified protein. Journal of
31 Biological Chemistry 276(52), 48644-48654.

32
33 Jayasena, S.D., 1999. Aptamers: An emerging class of molecules that rival antibodies in
34 diagnostics. Clinical chemistry 45(9), 22.

35
36 Jenison, R.D., Gill, S.C., Pardi, A., Polisky, B., 1994. High-Resolution molecular discrimination by
37 RNA. Science 263(5152), 1425-1429.

38
39 Kaatz, M., Schulze, H., Ciani, I., Lisdat, F., Mount, A.R., Bachmann, T.T., 2012. Alkaline
40 phosphatase enzymatic signal amplification for fast, sensitive impedimetric DNA detection.
41 Analyst 137(1), 59-63.

42
43 Kotia, R.B., Li, L., McGown, L.B., 2000. Separation of Nontarget Compounds by DNA Aptamers.
44 Analytical Chemistry 72(4), 827-831.

45
46 Lee, M., Walt, D.R., 2000. A fiber-optic microarray biosensor using aptamers as receptors.
47 Analytical Biochemistry 282(1), 142-146.

48
49 Lermo, A., Campoy, S., Barbé, J., Hernández, S., Alegret, S., Pividori, M.I., 2007. In situ DNA
50 amplification with magnetic primers for the electrochemical detection of food pathogens.
51 Biosensors and Bioelectronics 22(9-10), 2010-2017.

Loo, A.H., Bonanni, A., Ambrosi, A., Poh, H.L., Pumera, M., 2012. Impedimetric immunoglobulin G immunosensor based on chemically modified graphenes. *Nanoscale* 4(3), 921-925.

McDonald, J.R., 1987. *Impedance Spectroscopy*. John Wiley, New York.

Ocaña, C., Del Valle, M., 2014. Signal amplification for thrombin impedimetric aptasensor: Sandwich protocol and use of gold-streptavidin nanoparticles. *Biosensors and Bioelectronics* 54, 408-414.

Ocaña, C., Pacios, M., del Valle, M., 2012. A Reusable Impedimetric Aptasensor for Detection of Thrombin Employing a Graphite-Epoxy Composite Electrode. *Sensors* 12(3), 3037-3048.

Patel, D.J., Suri, A.K., 2000. Structure, recognition and discrimination in RNA aptamer complexes with cofactors, amino acids, drugs and aminoglycoside antibiotics. *Reviews in Molecular Biotechnology* 74(1), 39-60.

Radi, A., Acero Sánchez, J.L., Baldrich, E., O'Sullivan, C.K., 2005. Reusable Impedimetric Aptasensor. *Analytical Chemistry* 77(19), 6320-6323.

Sivasankar, S., Subramaniam, S., Leckband, D., 1998. Direct molecular level measurements of the electrostatic properties of a protein surface. *Proceedings of the National Academy of Sciences* 95(22), 12961-12966.

Song, W., Li, H., Liang, H., Qiang, W., Xu, D., 2014. Disposable electrochemical aptasensor array by using in situ DNA hybridization inducing silver nanoparticles aggregate for signal amplification. *Analytical Chemistry* 86(5), 2775-2783.

Srijanto, B.R., Cheney, C.P., Hedden, D.L., Gehl, A.C., Crilly, P.B., Huestis, M.A., Ferrell, T.L., 2012. Piezoresistive Microcantilevers-Based Cocaine Biosensors. *Sensor Letters* 10(3-4), 850-855.

Vasilescu, A., Gaspar, S., Mihai, I., Tache, A., Litescu, S.C., 2013. Development of a label-free aptasensor for monitoring the self-association of lysozyme. *Analyst* 138(12), 3530-3537.

Williams, E., Pividori, M.I., Merkoçi, A., Forster, R.J., Alegret, S., 2003. Rapid electrochemical genosensor assay using a streptavidin carbon-polymer biocomposite electrode. *Biosensors and Bioelectronics* 19(3), 165-175.

Yuan, J., Wu, S., Duan, N., Ma, X., Xia, Y., Chen, J., Ding, Z., Wang, Z., 2014. A sensitive gold nanoparticle-based colorimetric aptasensor for *Staphylococcus aureus*. *Talanta* 127(0), 163-168.

Zhang, J., Chai, Y., Yuan, R., Yuan, Y., Bai, L., Xie, S., 2013. A highly sensitive electrochemical aptasensor for thrombin detection using functionalized mesoporous silica@multiwalled carbon nanotubes as signal tags and DNAzyme signal amplification. *Analyst* 138(22), 6938-6945.

Zheng, Y., Chai, Y., Yuan, Y., Yuan, R., 2014. A pseudo triple-enzyme electrochemical aptasensor based on the amplification of Pt-Pd nanowires and hemin/G-quadruplex. *Analytica Chimica Acta* 834(0), 45-50.

Table 1. Summary of calibration results for the three amplification methods.

Amplification strategy	Sensitivity (M ⁻¹)	*RSD (%)	Detection limit (pM)	Amplification time (min)	Amplification factor %	Linear Range (pM)
Silver enhancement	2.2·10 ⁻¹⁴	9.9	0.30	7	89	0.1-100
Gold enhancement	2.0·10 ⁻¹⁴	8.8	0.45	4	80	0.1-100
Insoluble product reaction	7.0·10 ⁻¹⁴	11	0.30	15	189	0.1-100

* Corresponding to five replicate experiments at 75pM thrombin.

Figure Captions

Figure 1. Scheme of the experimental procedures of the three amplification strategies.

Figure 2. Insoluble product reaction.

Figure 3. Nyquist diagrams of: a) silver enhancement treatment, b) gold enhancement treatment and c) insoluble product reaction. ● bare AvGEC electrode, ○ biotinylated aptamer of thrombin 1, ▼ biotinylated aptamer of thrombin and thrombin protein, Δ sandwich complex, ■ sandwich complex modified with strep-AuNPs or av-HRP, □ sandwich complex modified with strep-AuNPs and silver enhancement treatment or modified with av-HRP and insoluble reaction. All experiments were performed in PBS solution and all EIS measurements were performed in PBS solution containing 0.01M $K_3[Fe(CN)_6]/K_4[Fe(CN)_6]$.

Figure 4. Regression curves of: a) silver enhancement treatment, b) gold enhancement treatment and c) insoluble product reaction. (1) (black circle) biotinylated aptamer of thrombin 1, (2) (white circle) sandwich complex, (3) (black triangle) sandwich complex modified with strep-AuNPs or av-HRP, (4) (white triangle) sandwich complex modified with strep-AuNPs and silver enhancement treatment. All experiments were performed in PBS solution and all EIS measurements were performed in PBS solution containing 0.01M $K_3[Fe(CN)_6]/K_4[Fe(CN)_6]$. Uncertainty values corresponding to replicated experiments (n = 5).

Figure 5. SEM images of: a.1) experiment using biotinylated aptamer of thrombin 1 + thrombin + biotinylated aptamer of thrombin 2 + strep-AuNPs + silver enhancement treatment, a.2) experiment using biotinylated aptamer of thrombin 1 + thrombin + biotinylated aptamer of cytochrome c + strep-AuNPs + silver enhancement treatment, b.1) experiment using biotinylated aptamer of thrombin 1 + thrombin + biotinylated aptamer of thrombin 2 + strep-AuNPs + gold enhancement treatment and b.2) experiment using biotinylated aptamer of thrombin 1 + thrombin + biotinylated aptamer of cytochrome c + strep-AuNPs + gold enhancement treatment. SEM images were taken at a acceleration voltage of 3 KV and a resolution of 2 μm .

Figure 6. 3D bar chart of the three amplifications methods response towards different proteins present in serum. Uncertainty values corresponding to replicated experiments (n = 5).

Figure 1

[Click here to download high resolution image](#)

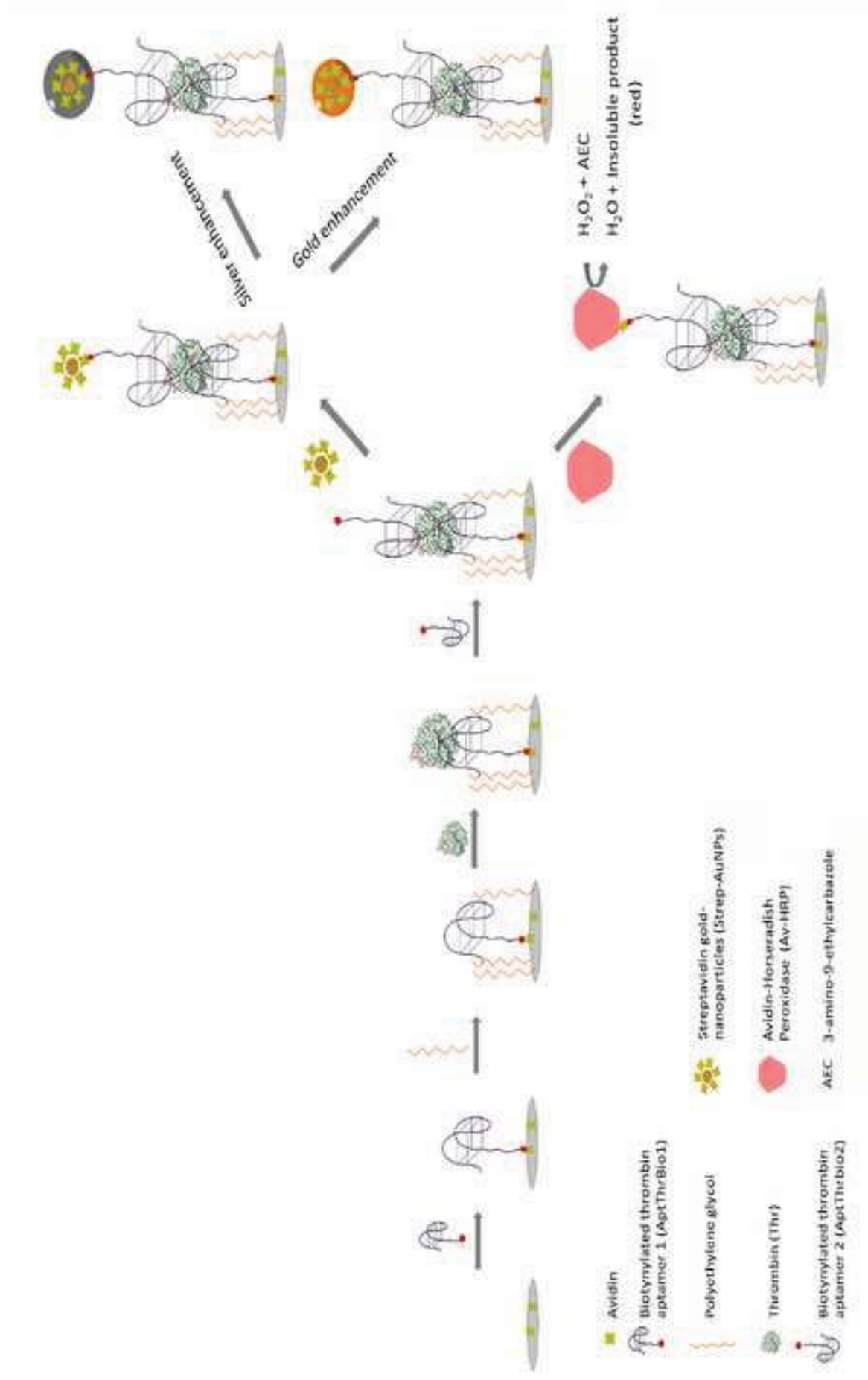


Figure 2
[Click here to download high resolution image](#)

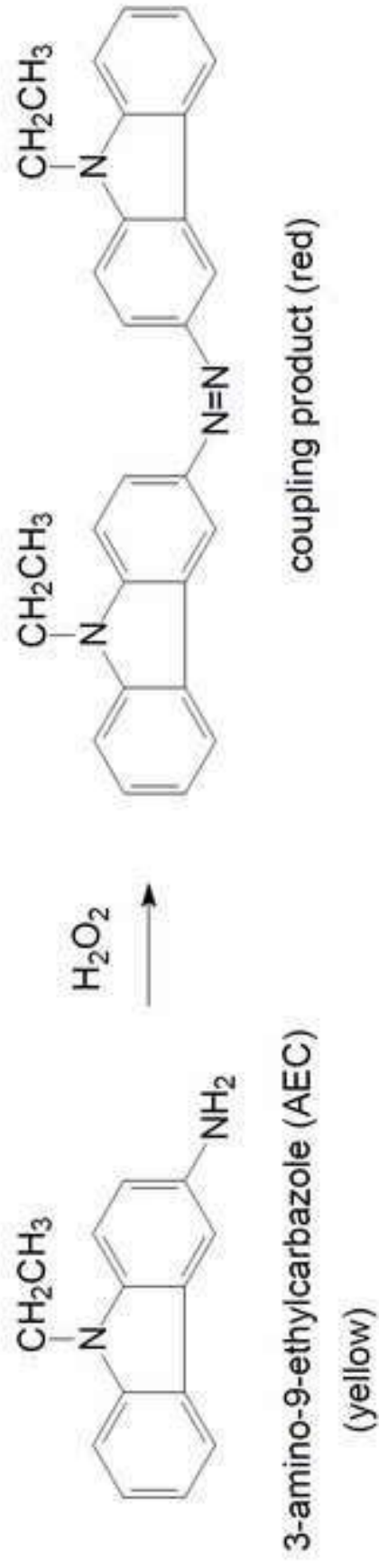


Figure 3

[Click here to download high resolution image](#)

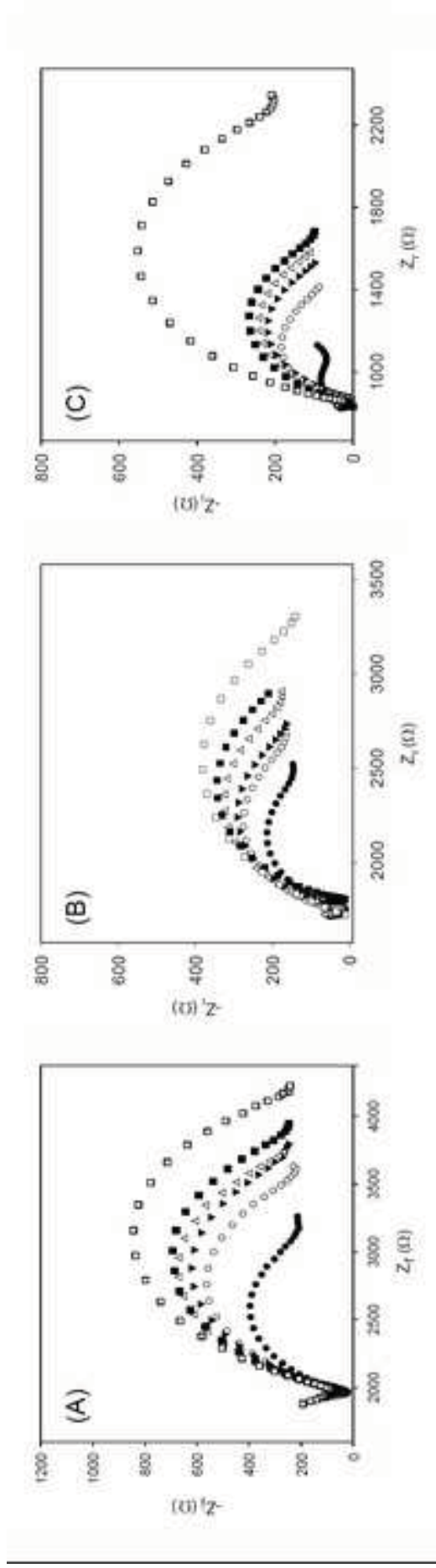


Figure 4

[Click here to download high resolution image](#)

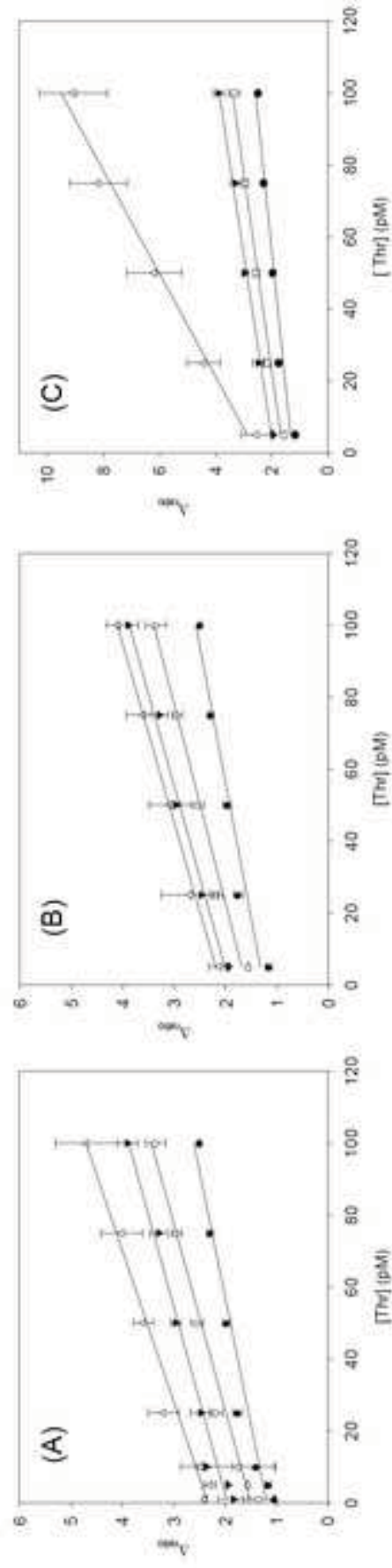


Figure 5
[Click here to download Figure: Figure 5.pdf](#)

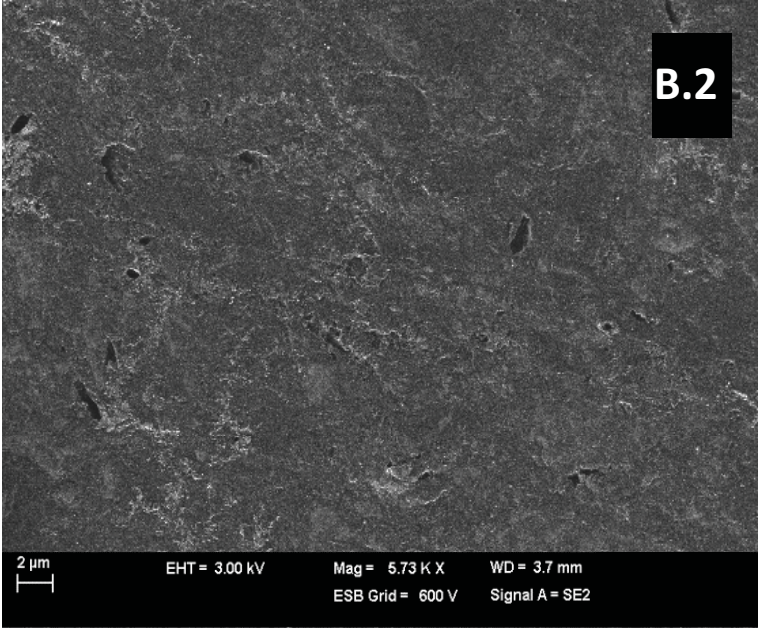
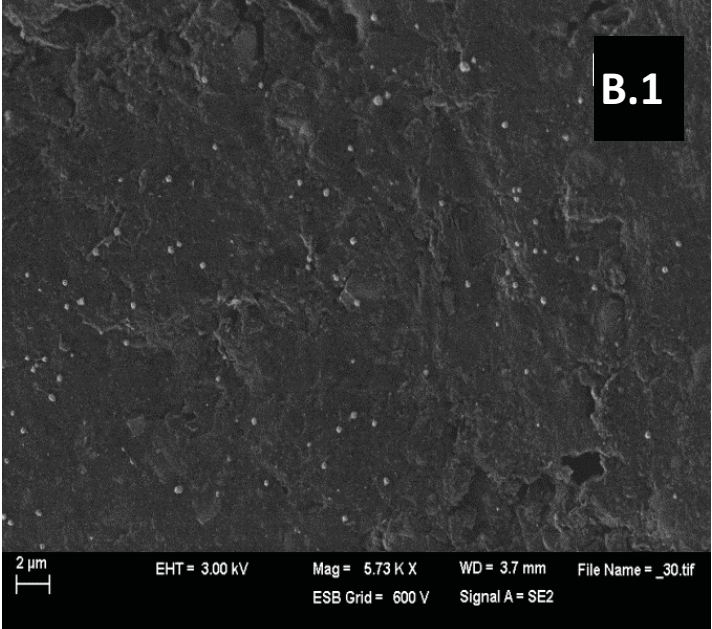
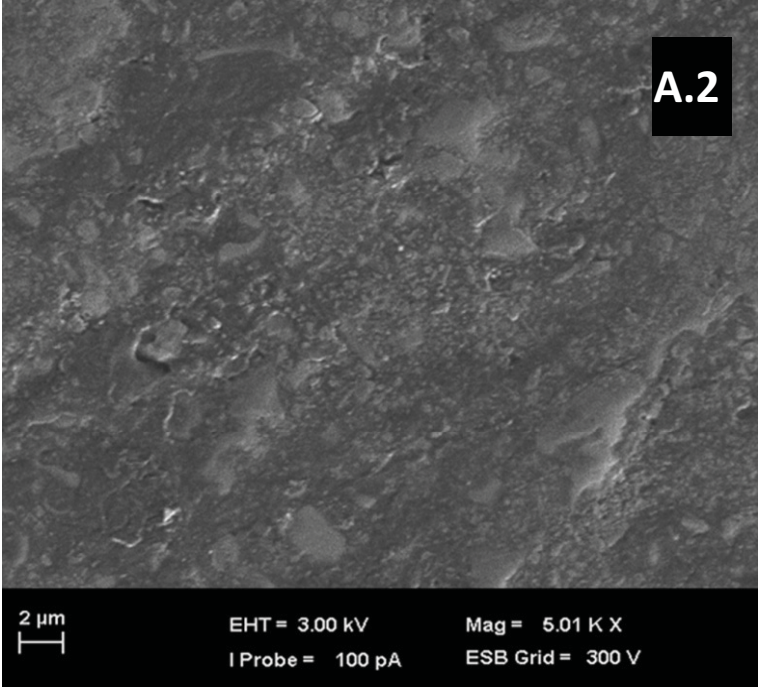
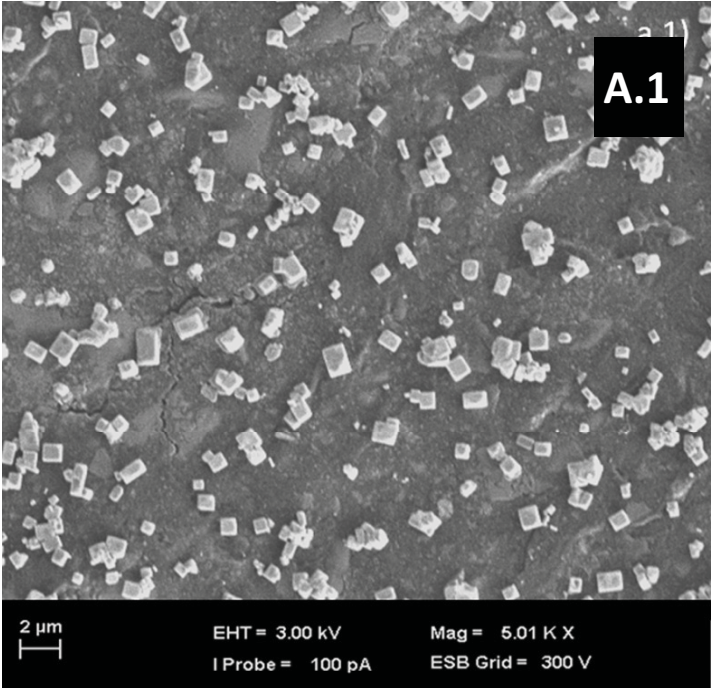


Figure 6
[Click here to download high resolution image](#)

